CHALMERS UNIVERSITY OF TECHNOLOGY **CHARMEC**
Mechanics and Maritime Sciences **Chalmers Railway Mechanics**

Tore Vernersson
Anders Ekberg
Roger Lundén

Lina Andersson
Transportstyrelsen

2019-06-13
24 pages

Swedish tests of block brake performance in winter conditions

Winter 2017-2018

Detailed analyses of experimental results

Summary

Data from the Swedish tests on LL brake blocks, performed in March and April 2018, have been analysed in detail by merging tabulated data on brake cycles with measured hanger link forces for the individual braking cycles. The time average of the hanger link forces are compared for a wheelset with cast iron blocks and a wheelset with LL brake blocks, being organic composite brake blocks IB116* or sinter brake blocks C952-1. The average forces are also related to brake pressures for establishing a ratio that mimics the variation of the coefficient of friction. It should however be noted that the geometrical positions of the hanger links, which is affected by the wear state of wheels and of brake blocks, has an influence on this value. No compensation has been made to find the actual friction force acting on the wheel. Finally, the time of onset of the friction force for each insert is assessed in order to study the time delay for the brake blocks.

For the studied clasp brake block arrangement, the forces in the hanger links that are loaded in tension are first assessed and after this the forces of the hanger links that are loaded in compression. A reason for separating the analyses in this way is that the forces have different characteristics. For instance, the tensioned hanger links have a relatively high magnitude whereas the compressed hanger links have a low magnitude.

For the hanger links in tension, one main results is that according to the relation between hanger link force and brake pressure, the organic composite brake block and the sinter blocks exhibit clearly lower hanger link forces than do cast iron blocks. In fact, when considering average braking performance, the organic composite brake block provides 82% of the friction force given by the cast iron blocks for a given brake pressure and the sinter block provides 75% of the friction force for cast iron blocks. Comparison with winter conditions for non-snowy conditions indicate that the value for the organic composite is typical, thus not depending on snow conditions. Another key issue is the variability of the braking performance of the LL brake blocks as compared to the one of the cast iron brake blocks. It is found that the standard deviations in the hanger link forces are somewhat lower for the organic composite brake blocks than for cast iron blocks and the value for sinter blocks are even lower than that. The time delay for the onset of the friction forces is generally short and the differences between the block types is minor.

For the hanger links that are loaded in compression by the frictional forces, it was found that a large number of brake cycles nevertheless give average hanger link forces that are tensile. This is an indication on that the friction forces have not developed properly between block and wheel for the studied brake cycle. Based on this, an analysis of the time delay was performed, with the delay taken as time from start of braking until the moment of onset of the friction forces in each studied hanger link (taken as the instance when the individual compressive force reached 10% of the value of the most compressive force during the cycle). It was found that organic composite blocks had the longest delays, followed by sinter blocks and cast iron blocks.

Contents

1. Background and Aim

The present study reports on a detailed assessment of data from the Swedish winter tests on cast iron and LL-type brake blocks as tested during some days in March and April 2018. The analyses are based on the data given in the test report[1] and the data files that were acquired during the tests[2]. To this end, data have been read into Matlab to allow for easy processing, structuring and visualization of results.

2. Method

Firstly, the data in Appendix A of the test report were read into Matlab, providing the following useful data for individual brake cycles: date and time, initial speed of braking, end speed of braking and braking pressure. In addition, comments are given on weather conditions regarding snow. After this, each individual brake cycle was identified in the data files by a procedure based on 1) finding the approximate time period using supplied time marks, and 2) to manually mark beginning and end of each brake cycle. For each identified brake cycle, the signals of the force transducers were put to zero just prior to the brake cycle, and the average force during braking[3] was calculated.

In the test report, the sensors (strain gauges) for forces in the hanger links are denoted 1-8, see Figure 1. In the present report, new names have been introduced as based on functioning. The two sensors 1 and 3, which should have the same nominal forces (being cast iron brake blocks acting under the same brake force), are denoted as "Cast Front" with additional designations "Left" and "Right" when they need detailing. In the same sense, sensors 2 and 4 are denoted "Casts Back" with additional "Left" and "Right". The same method are used for sensors 5 and 7 being "Front" of LL-braked wheelset. For this wheelset sometimes "OC" (for Organic Composite) is used for block IB116* or "S" for sinter block C952-1.

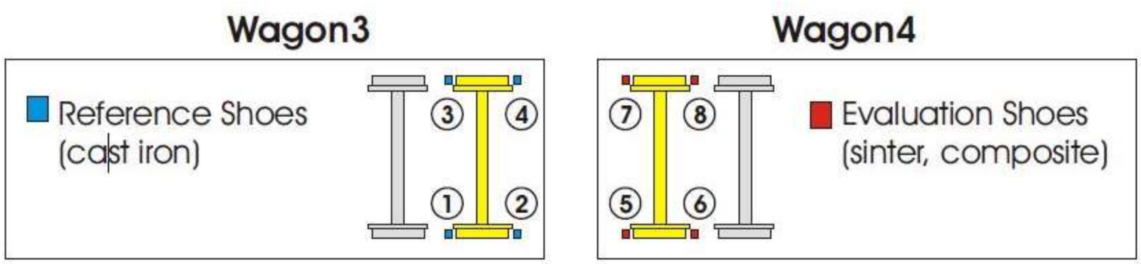

Figure 1 Sensor positions of hanger links in test train

[1] D. Larsson, Swedish tests of block brake performance in winter conditions, *Damill AB*, 2018-09-30, 20 pp

[2] Data files in xls-format sent by Lina Andersson, Transportstyrelsen to Tore Vernersson on 2018-12-04

[3] The average force was calculated for the duration of the braking cycle for which the total braking force is higher than 10% of the maximum braking force during the considered cycle.

3. RESULTS AND DISCUSSION

A total of 250 brake cycles could be identified, see Figure 2. It was found that the force sensor of one hanger link was not functioning at all during the tests (sensor 5 of the test-report, being one of the “front” hanger links for the LL-brake blocks). The test wagons are going either forward or backward during different stages of the test campaign. For this reason, the hanger links that are in tension varies during testing. It was found that the compressive forces sampled during testing often had problems relating to non-physical results (i.e they were indicated to be in tension). For this reason, the assessment in the present report first study forces in the hanger links that are in tension and after that the ones in compression are studied.

In order to investigate the frictional characteristics of the brake blocks, the ratio between the hanger link force and the (nominal) brake pressure is calculated, see Figure 3. Upon investigation, the pressure value given for brake cycle 34 is assumed incorrect, and the figure is for that reason re-scaled and presented in Figure 4.

The forces are really low for the initial tests (stops 1-16) and they are for this reason omitted from further analysis. In addition, the final cycles (stops 191-250) have lower forces for given pressures than the other cycles, indicating a difference in the amplifier settings during for these stops. Also these cycles are omitted if not explicitly stated otherwise.

Brake cycles 230-250 are for non-snowy runs when using IB116* on all axles of the test train, except for the reference wagon 3 that still had cast iron brake blocks. Note that these have a different relation between force and pressure due to an assumed difference in amplification settings for the force transducers as mentioned above.

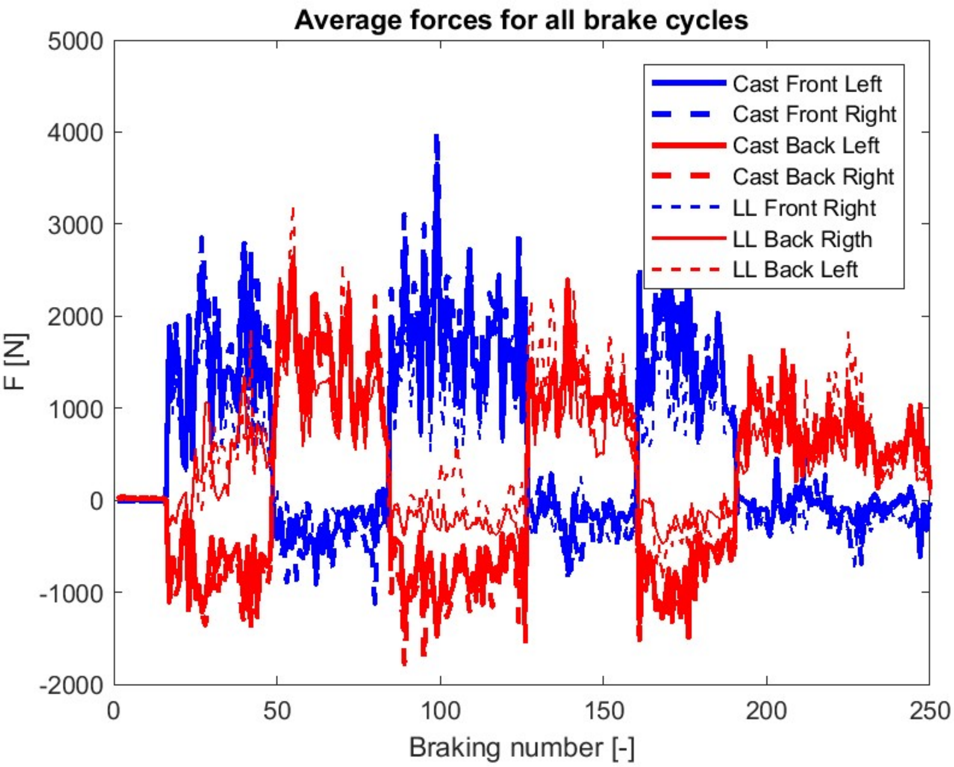

Figure 2 Average forces for hanger links of cast iron brake blocks and of LL-blocks for all 250 identified brake cycles

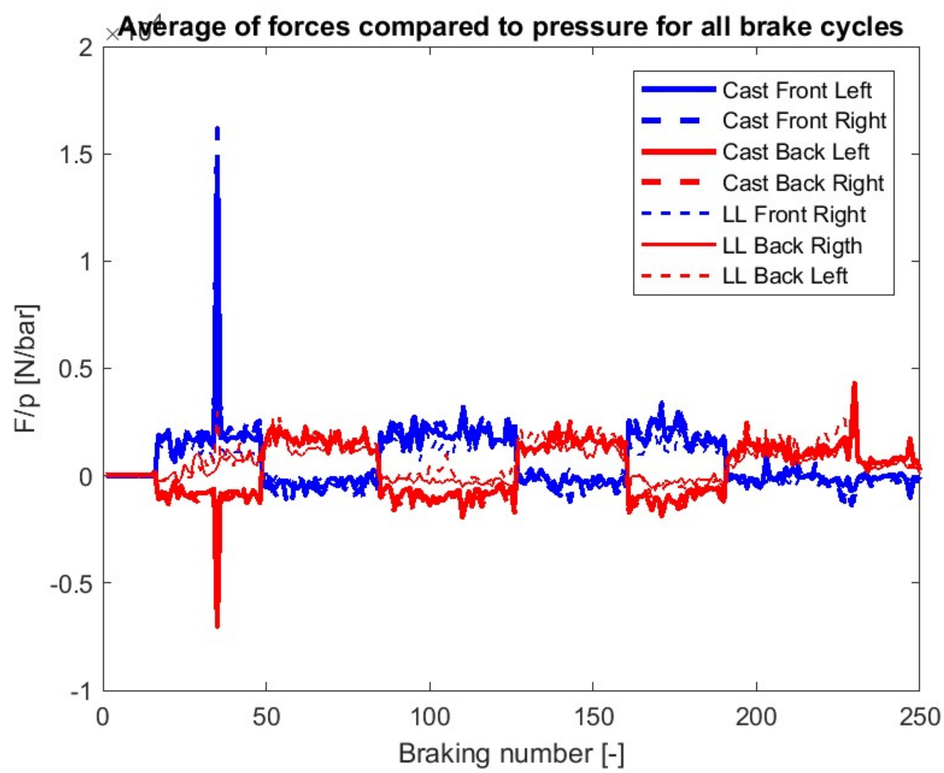

Figure 3 Ratio between average force in hanger links and brake pressure (Note multiplier 10^4 on vertical axle)

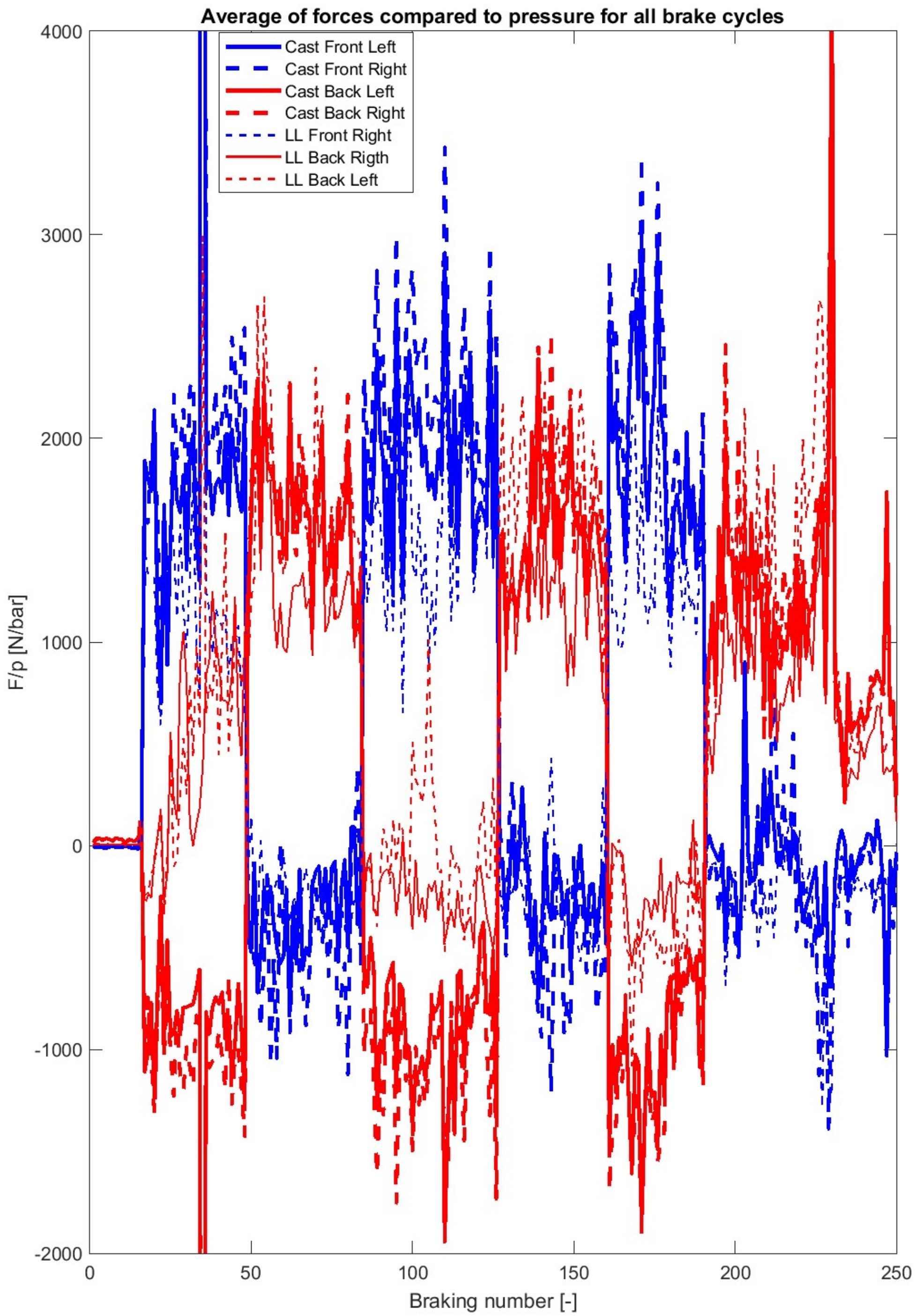

Figure 4 Ratio between average force in hanger links and brake pressure.

3.1. Hanger links in tension

The frictional behavior of the brake blocks is further investigated by dividing the hanger link force by the brake pressure, where the hanger link force is used as a representative of the true friction force[4] and the brake pressure is proportional to the brake (normal) force. The results in Figure 5 show a histogram over the occurrence of different ranges of forces over pressures for cast iron brake blocks and for tested LL brake blocks. The ratio is clearly larger for the cast iron brake blocks than for the LL blocks, pointing towards a lower coefficient of friction of these blocks than for the cast iron blocks during the winter tests. In Figure 6, LL-blocks have been split into organic composite and sinter types. For the organic composite blocks, there appears to be a larger spread in the results than for the sinter blocks.

Another way to investigate the friction behavior is to compare the forces of the LL block hanger links to the ones of the cast iron block hanger links for each of the brake cycles, see Figure 7 and Figure 8. In Figure 7 all brake cycles are included and in Figure 8 only the ones at performed at brake pressures higher than 0.8 bars. The histograms all indicate that the LL-type brake blocks generally give a lower force in the hanger links than the cast iron brake blocks.

In Figure 9, the relation between hanger link force and brake pressure is visualized for all brake cycles. In addition, a linear polynomial is fitted to the data points[5]. The slopes of the curves indicate that the hanger link force for the organic composite brake blocks is 82% of the one for cast iron[6]. The ratio for sinter blocks is 75%[7]. The standard deviations of the data are similar for the organic composite and the cast iron material, being 390 N and 366N respectively, whereas it is somewhat lower for the sinter material at 295 N.

In Figure 10, the relation between hanger link force and brake pressure is visualized only for the final cycles of the organic composite brake block which were for non-winter conditions (cycles 230-250). Again, a linear polynomial is fitted to the data points. The slopes of the curves indicate that the hanger link force for the organic composite brake blocks is 81 % of the one for cast iron[8]. This value is actually lower than for the result 85% for which winter conditions were considered in the paragraph above. The standard deviation is here 188 N for the cast iron brake block and 152 N for the organic composite. These two latter values needs scaling to allow for comparison with the data for winter conditions. If we assume that the cast iron slopes should be the same, it means that the values should be increased by the ratio 1861/708.6 = 2.63, resulting in standard deviation 494 N for the cast iron blocks and 399 for

---

[4] The angle between the hanger link and the tangential direction of the block contact on the tread is here unknown (not measured at the tests). Assuming a similar degree of wear for the different block types should correspond to similar angles and the error upon comparison should then be small.

[5] A linear polynomial fit without intercept was chosen.

[6] Ratio organic composite vs cast iron (1523 [N/bar] / 1861 [N/bar])

[7] Ratio sinter vs cast iron (1390 [N/bar] / 1861 [N/bar])

[8] Ratio organic composite vs cast iron (573.1 [N/bar] / 708.6 [N/bar])

the organic composite blocks. These standard deviations are both higher than the ones found for the winter conditions as discussed in the previous paragraph.

Additionally, the time delay from start of braking until onset of the frictional forces for each of the brake block inserts was investigated. The onset of the force was defined as the duration after start of braking when the individual hanger link force reached 10% of its maximum value for the individual brake cycle. The results are presented for cast iron in Figure 11, organic composite and sinter blocks in Figure 12. The time delays are small in general, below some 7 s for all but 2 cycles. The time history of the hanger link signals for these two cycles are Figure 13. It can be seen that these cycles are most likely braked using a brake pressure that is initially low and only increasing to full magnitude after a prolonged time of the studied cycles. However, since no data for the brake pressure signal is available from tests, this remains a hypothesis.

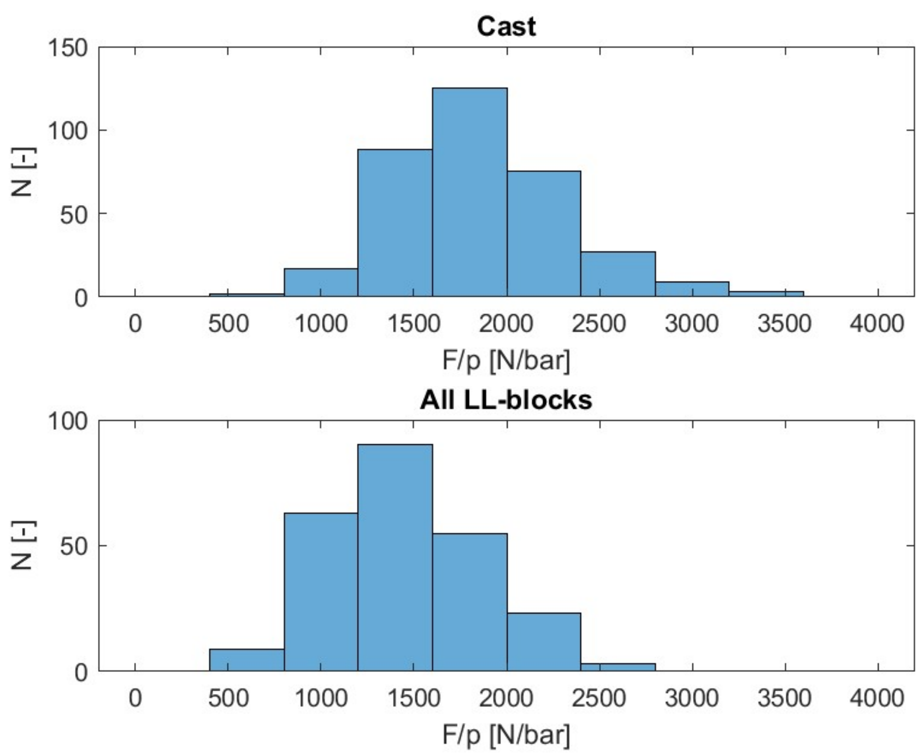

Figure 5 Histogram of number of brake cycles related to average force in hanger links divided by brake pressure. Results from higher amplifier setting (cycle 191-250 are excluded).

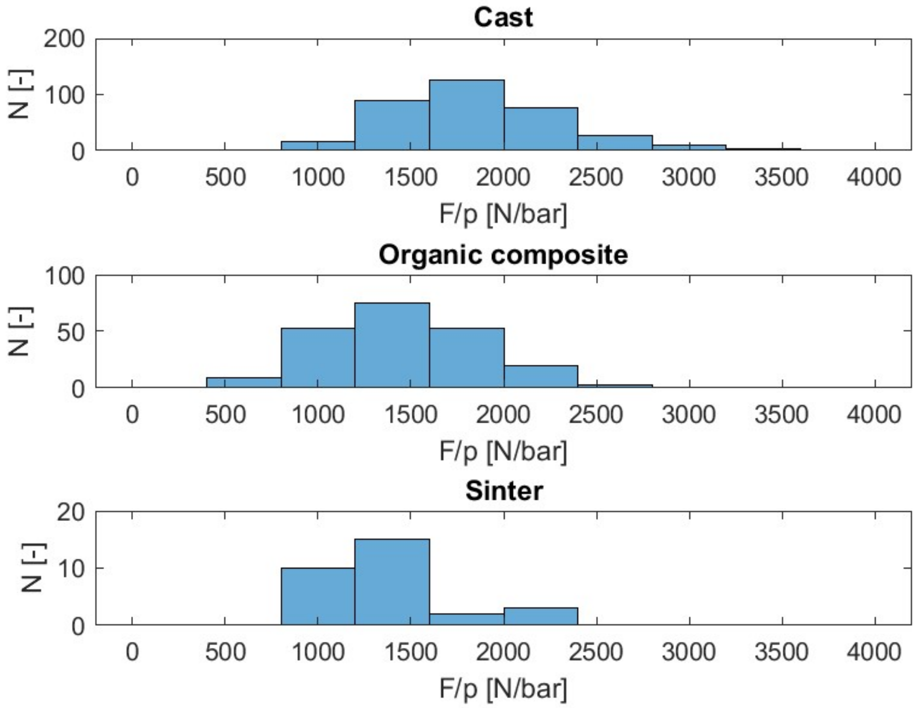

Figure 6 Histogram of number of brake cycles related to average force in hanger links divided by brake pressure. Results from higher amplifier setting (cycle 191-250 are excluded).

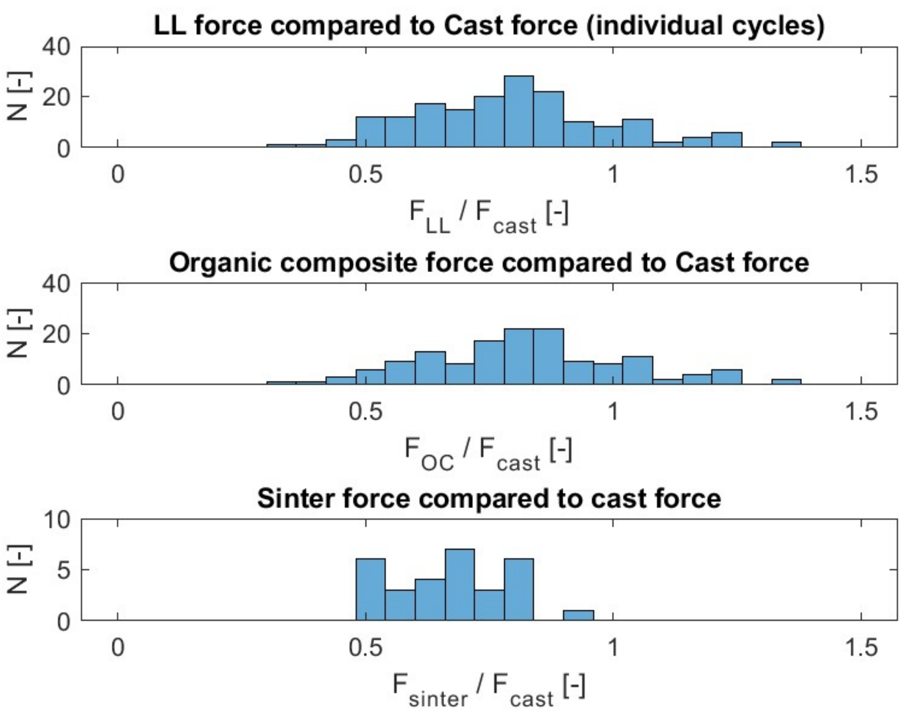

Figure 7 Histogram of number of brake cycles related to force of LL-blocks divided by force on Cast blocks (for individual cycles)**.** Results from higher amplifier setting (cycle 191-250 are excluded).

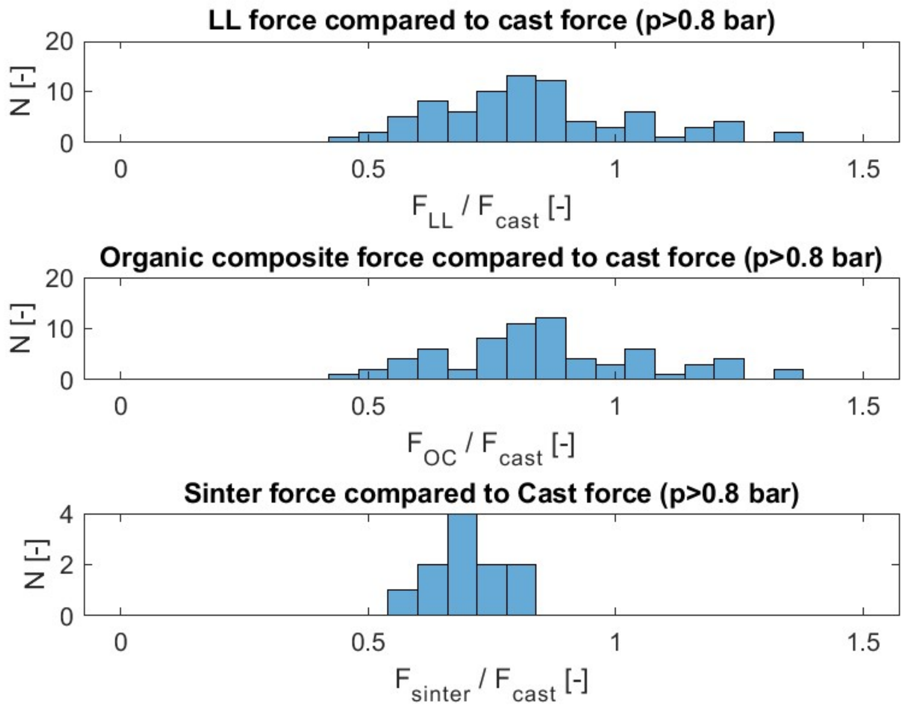

Figure 8 Histogram of number of brake cycles related to force of LL-blocks divided by force on Cast blocks (for individual cycles). Data only for brake cycles with higher brake pressures. Results from higher amplifier setting (cycle 191-250 are excluded).

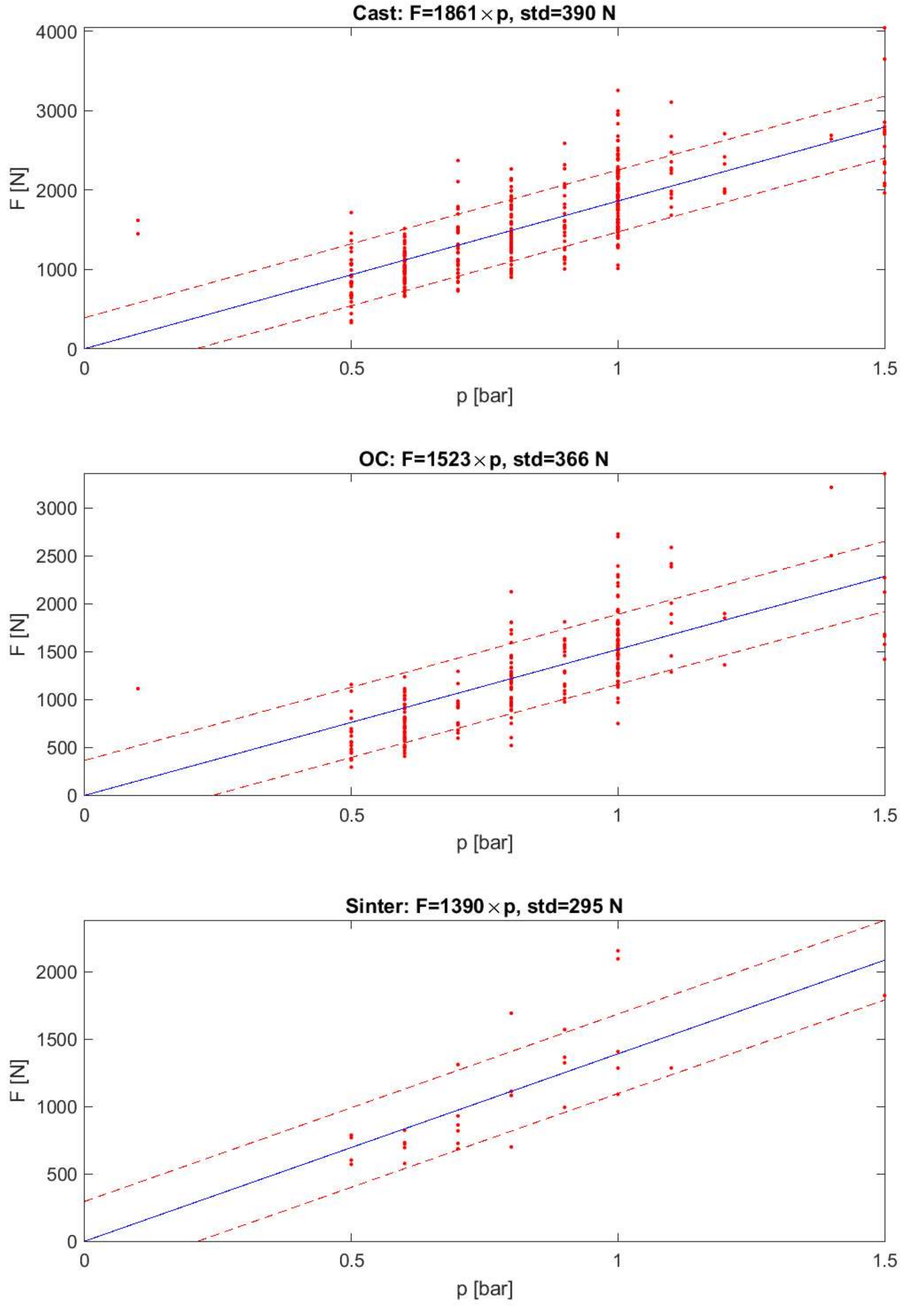

Figure 9 Hanger force as function of brake pressure for individual cycles along with fitted linear polynomial. Results from higher amplifier setting (cycle 191-250 are excluded).

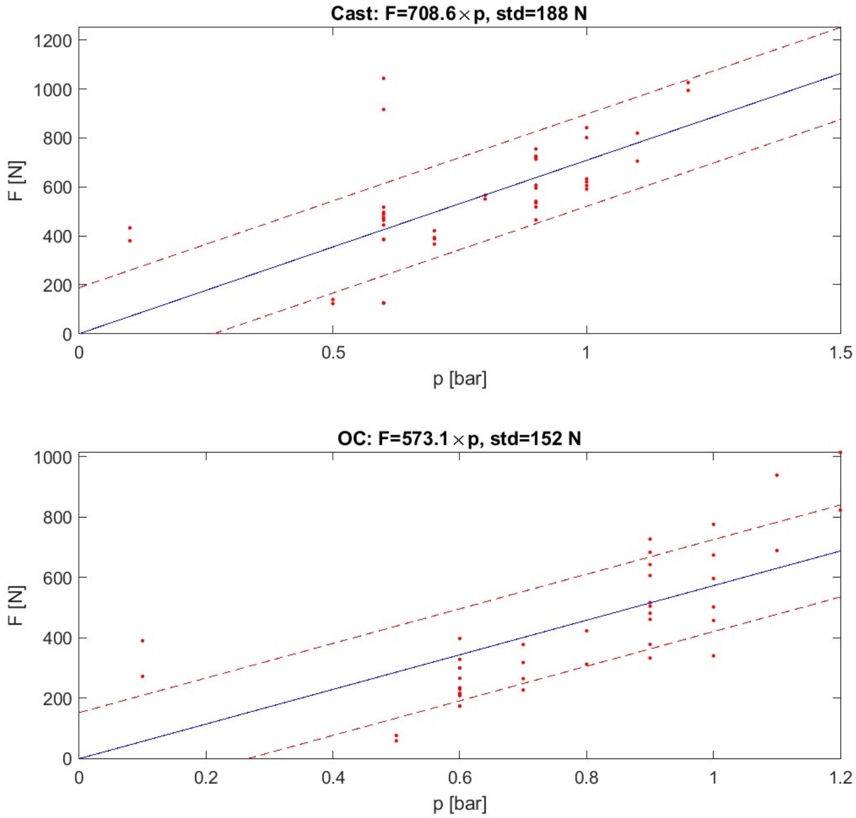

Figure 10 Hanger force as function of brake pressure for individual cycles along with fitted linear polynomial. Results only from April with IB116* when no winter conditions prevailed. Note that these results are from lower amplifier setting (only cycle 191-250).

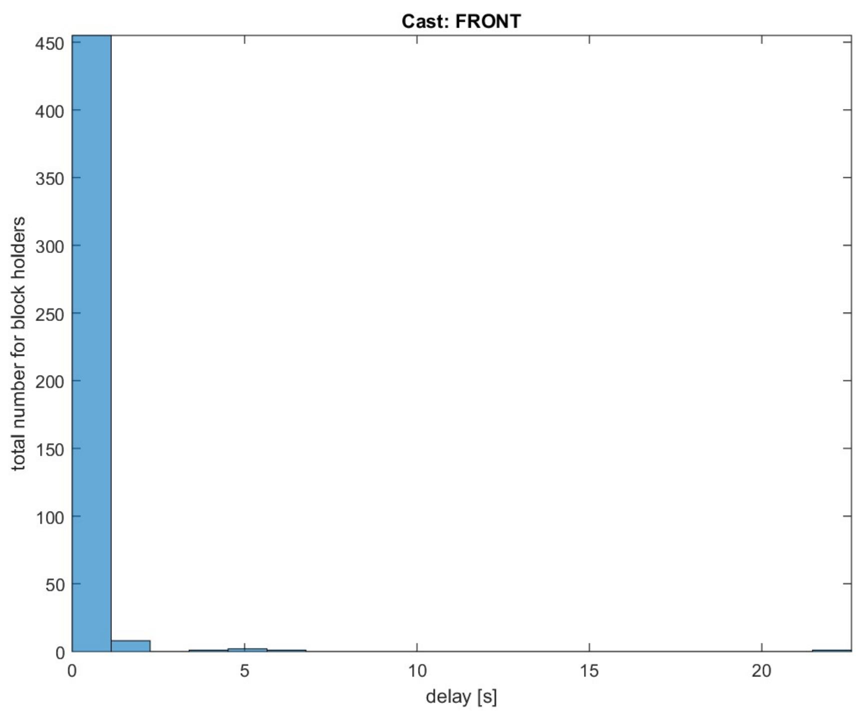

Figure 11 Histogram of number of brake cycles giving prescribed time delay from start of braking until onset of hanger link (friction) force for cast iron brake blocks

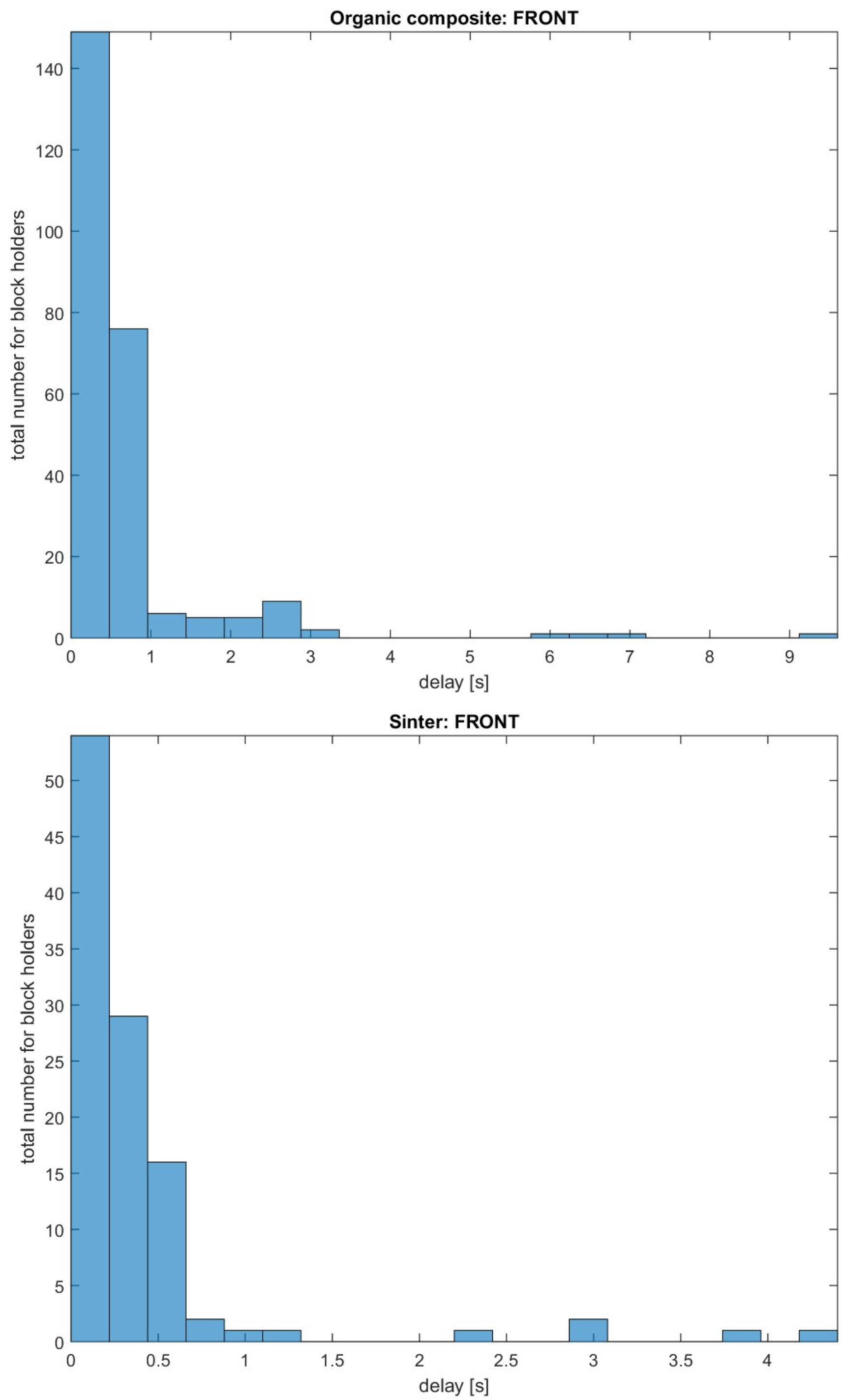

Figure 12 Histogram of number of brake cycles giving prescribed time delay from start of braking until onset of hanger link (friction) force for LL brake blocks. Results for organic composite at top and sinter at bottom. Note different scales on axes.

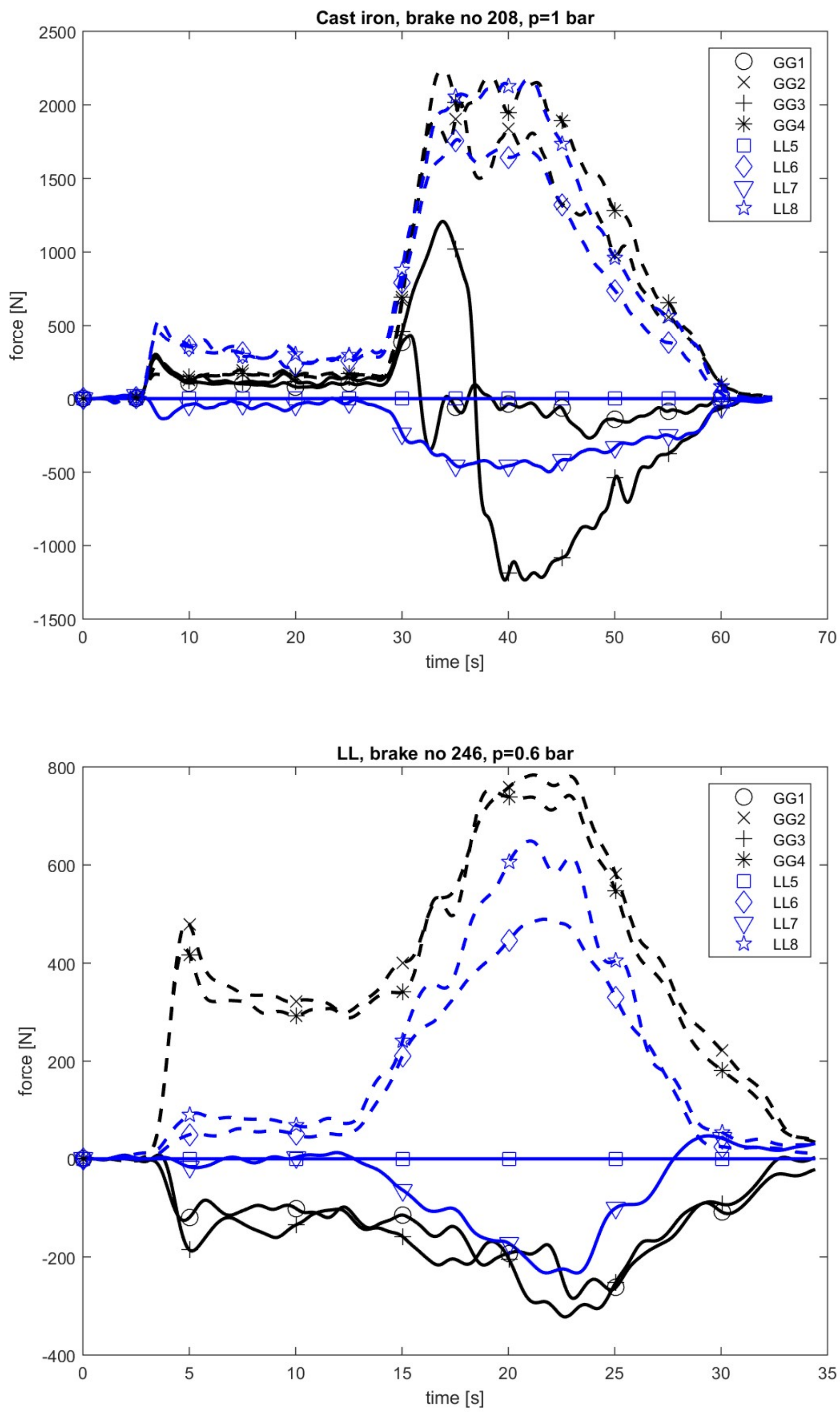

Figure 13 Time variation of forces for brake cycle with a high time delay until onset of friction forces for cast iron (top) and organic composite (bottom).

3.2. Hanger links in compression

The ratio between hanger force and the brake pressure, are presented in Figure 14 in the form of a histogram over the occurrence of different ranges of forces over pressures for cast iron brake blocks and for tested LL brake blocks. It can be noted that for the cast iron brake blocks almost all brake cycles provide a negative ration of force over pressure, which is appropriate for a hanger link in compression. However, for the LL blocks, there is a high number of cycles that gives an average force for the braking that is positive, yielding a force over pressure that is positive. This indicates a problem with how the friction force is acting on the wheel. For the hanger link force to be in tension it means that the friction force is not correctly manifested between brake block and wheel during a major part of the assessed stop braking cycle. Instead the tensile force in the hanger link is an effect of how the normal load on the block is taken by the hanger link. In Figure 15, LL-blocks have been split into organic composite and sinter types. For the organic composite blocks, there appears to be a number of braking cycles that produce such problematic positive forces than for the sinter blocks.

Instead of continuing the study of brake force over pressure, focus was instead put on the reason for the problematic tensile forces in the hanger links that should be compressed by the friction forces. A histograms over results of time delay for cast iron blocks are given Figure 16, and for organic composite and sinter blocks in Figure 17. Evident from the figures is that all brake block types can give large time delays until onset of the friction forces. However, a larger ratio of brake cycles give large time delays, higher than, say 10 s, for the organic composite blocks than for the other blocks types. In Figure 18 and in Figure 19, histograms are expanded to also give information on brake pressure. There is an indication that large time delays are more common for lower brake pressures, but one should not that there are only a few number of cycles at high brake pressure levels.

Two examples of time histories that give large time delays are given for in Figure 20, Figure 21 and Figure 22 for cast iron, organic composite and sinter blocks respectively.

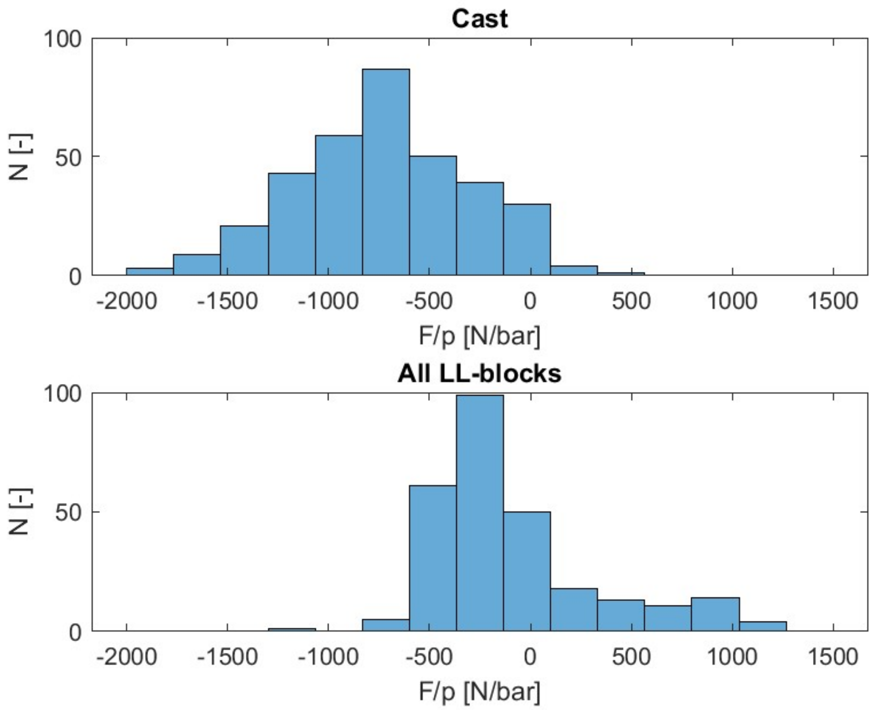

Figure 14 Histogram of number of brake cycles related to average force in hanger links divided by brake pressure. Results from higher amplifier setting (cycle 191-250 are excluded).

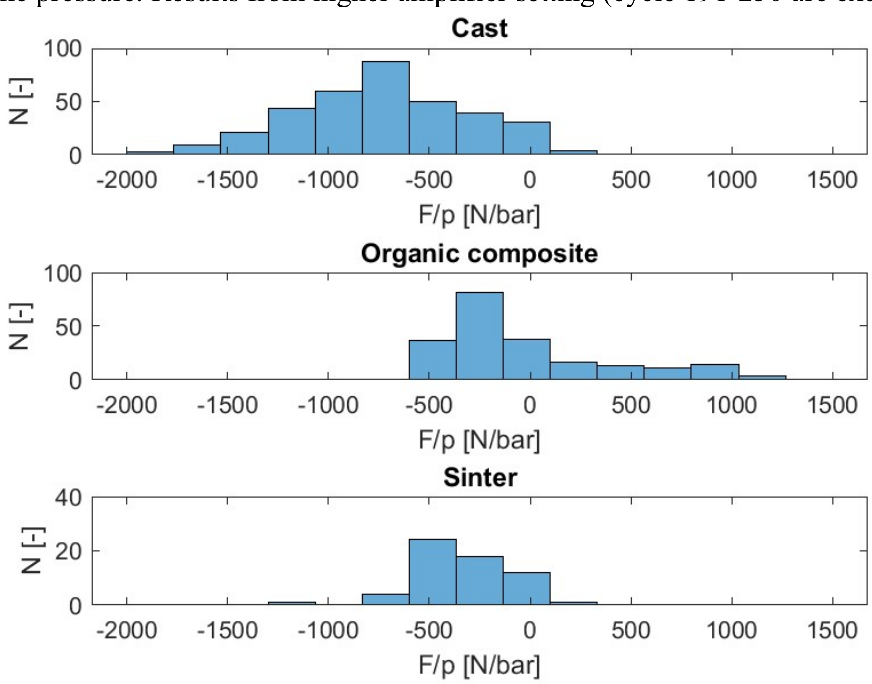

Figure 15 Histogram of number of brake cycles related to average force in hanger links divided by brake pressure. Results from higher amplifier setting (cycle 191-250 are excluded).

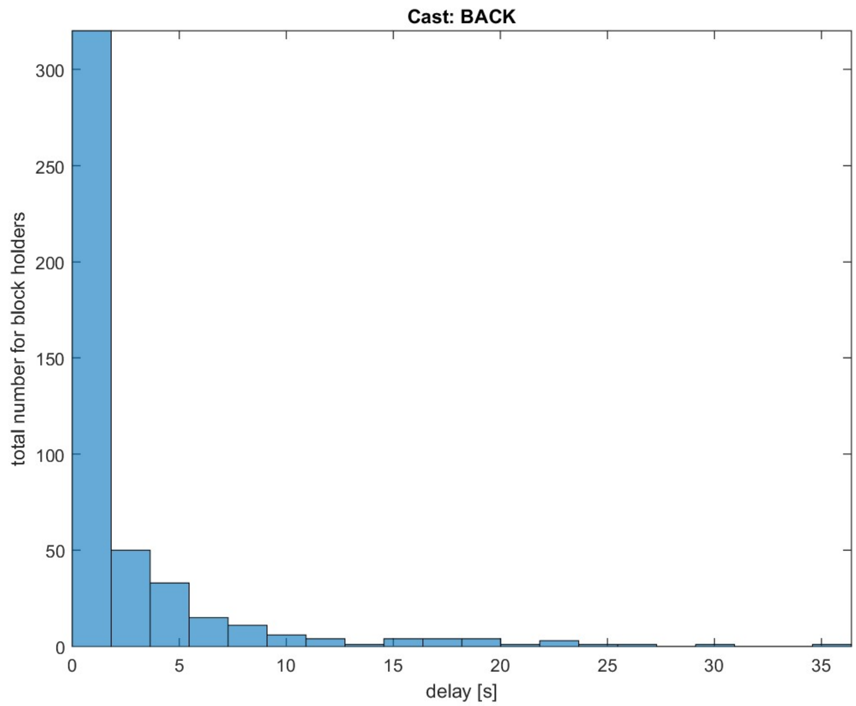

Figure 16 Histogram of number of brake cycles giving prescribed time delay from start of braking until onset of hanger link (friction) force for cast iron brake blocks

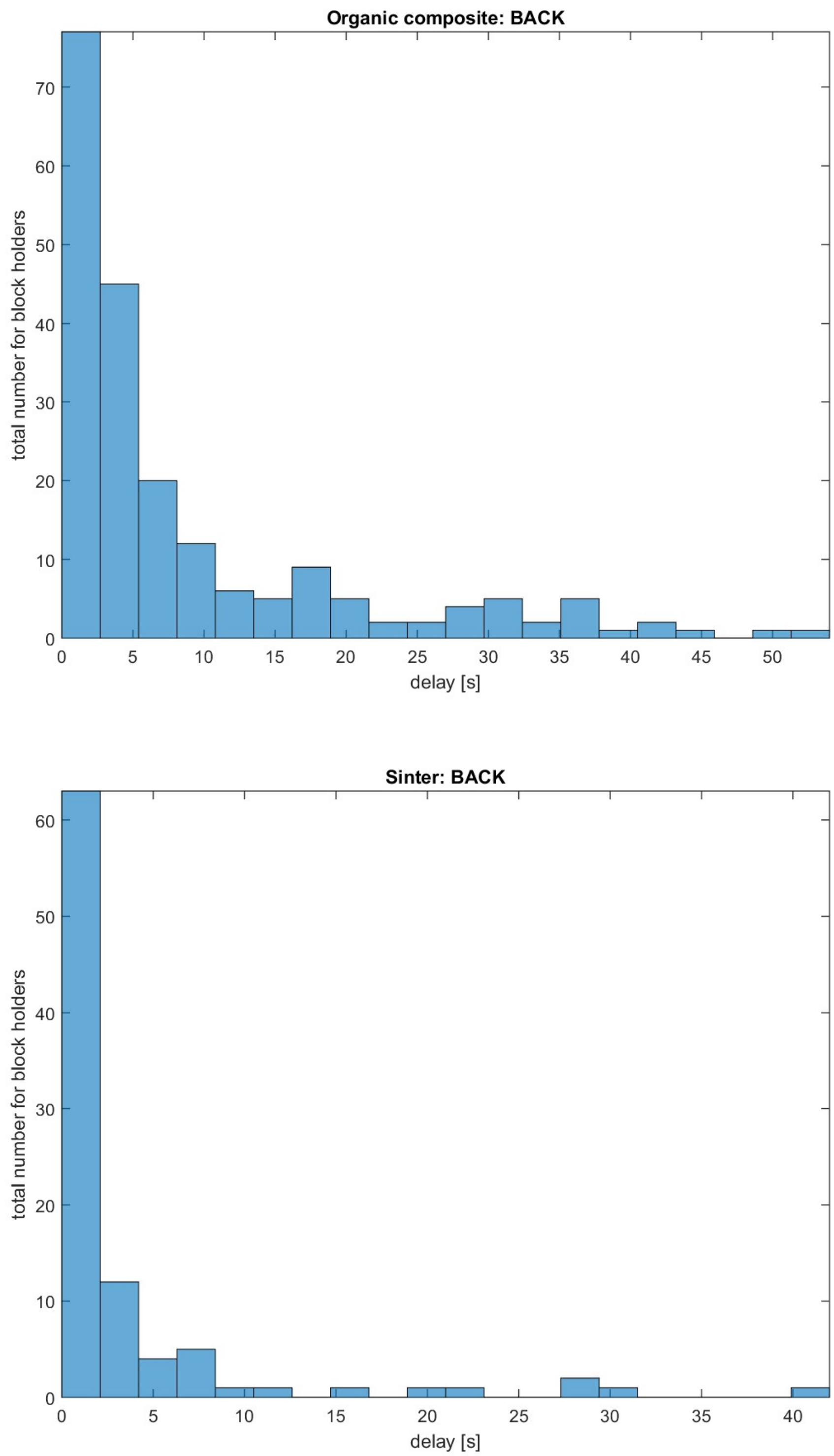

Figure 17 Histogram of number of brake cycles giving prescribed time delay from start of braking until onset of hanger link (friction) force for LL brake blocks. Results for organic composite at top and sinter at bottom. Note different scales on axes.

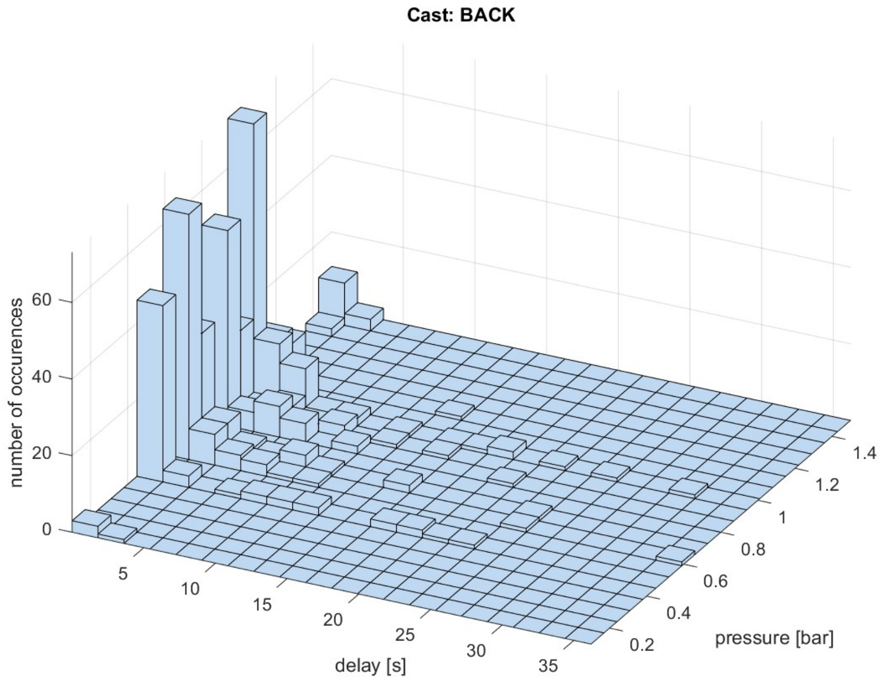

Figure 18 Histogram of number of brake cycles for given brake pressure and prescribed time delay from start of braking until onset of hanger link (friction) force for cast iron brake blocks

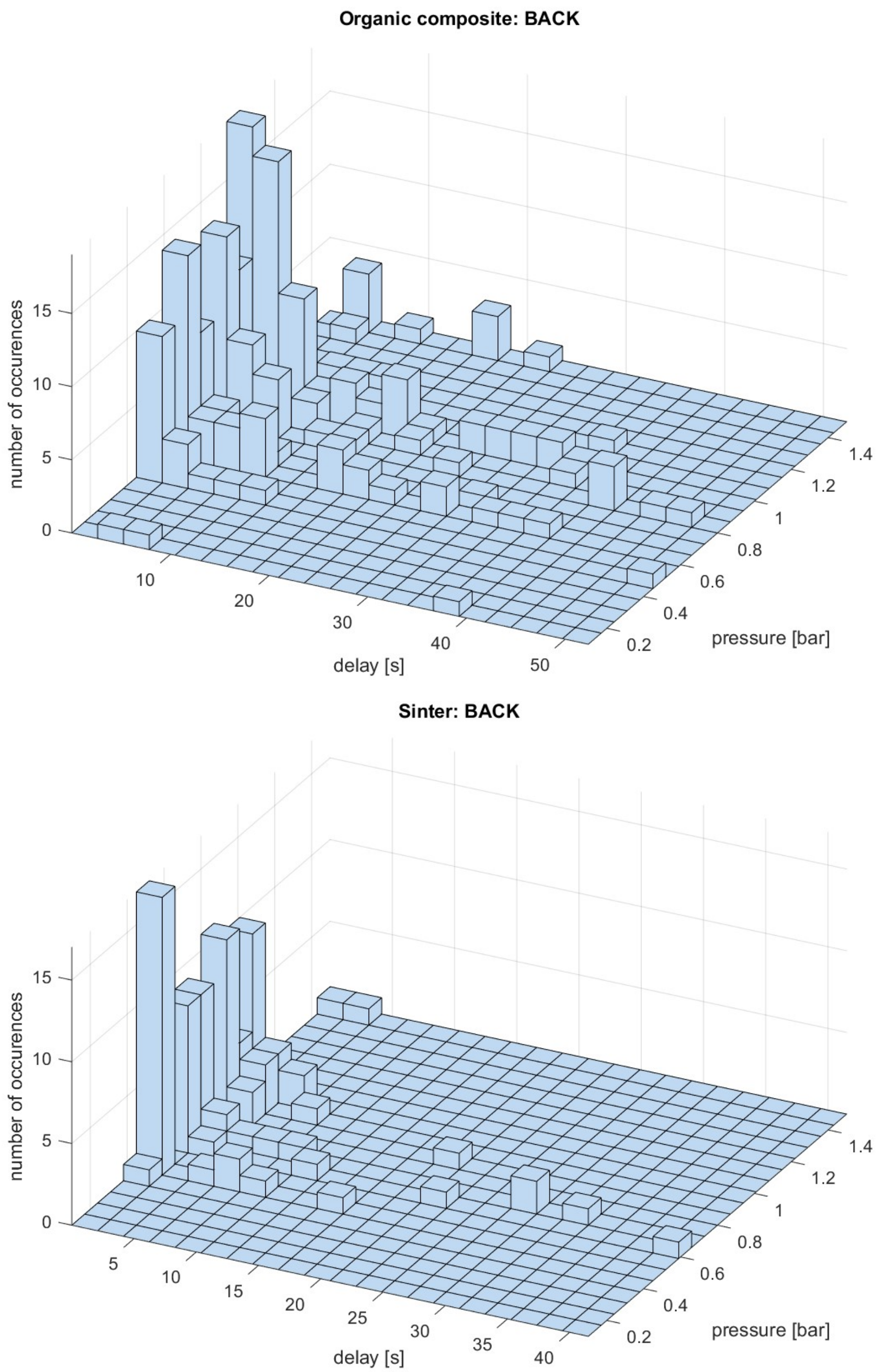

Figure 19 Histogram of number of brake cycles for given brake pressure and prescribed time delay from start of braking until onset of hanger link (friction) force for LL brake blocks. Results for organic composite at top and sinter at bottom. Note different scales on axes.

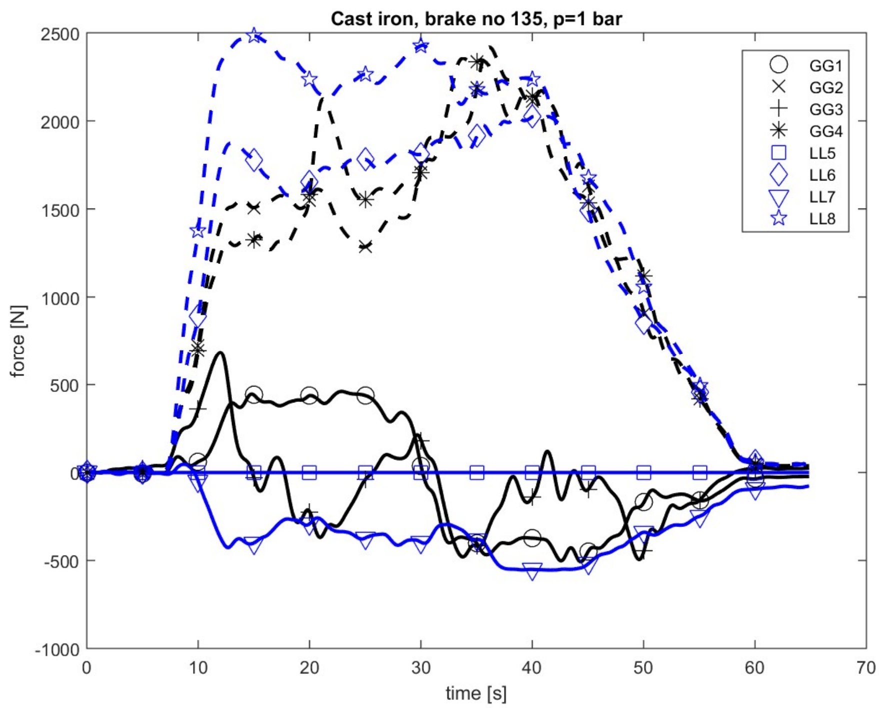

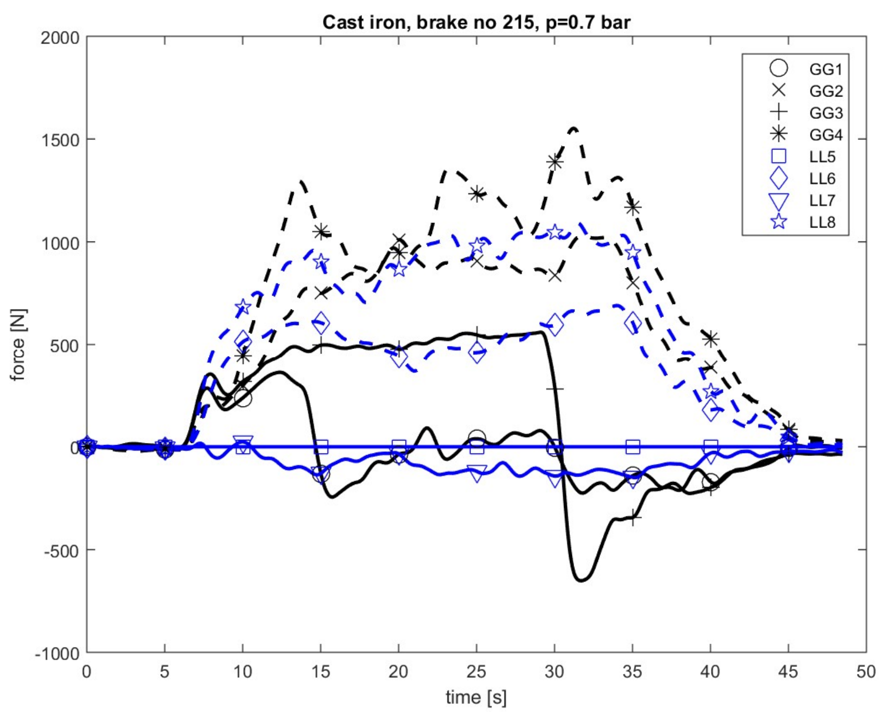

Figure 20 Two examples of time variation of forces for brake cycles with a high time delay until onset of friction forces for cast iron brake blocks.

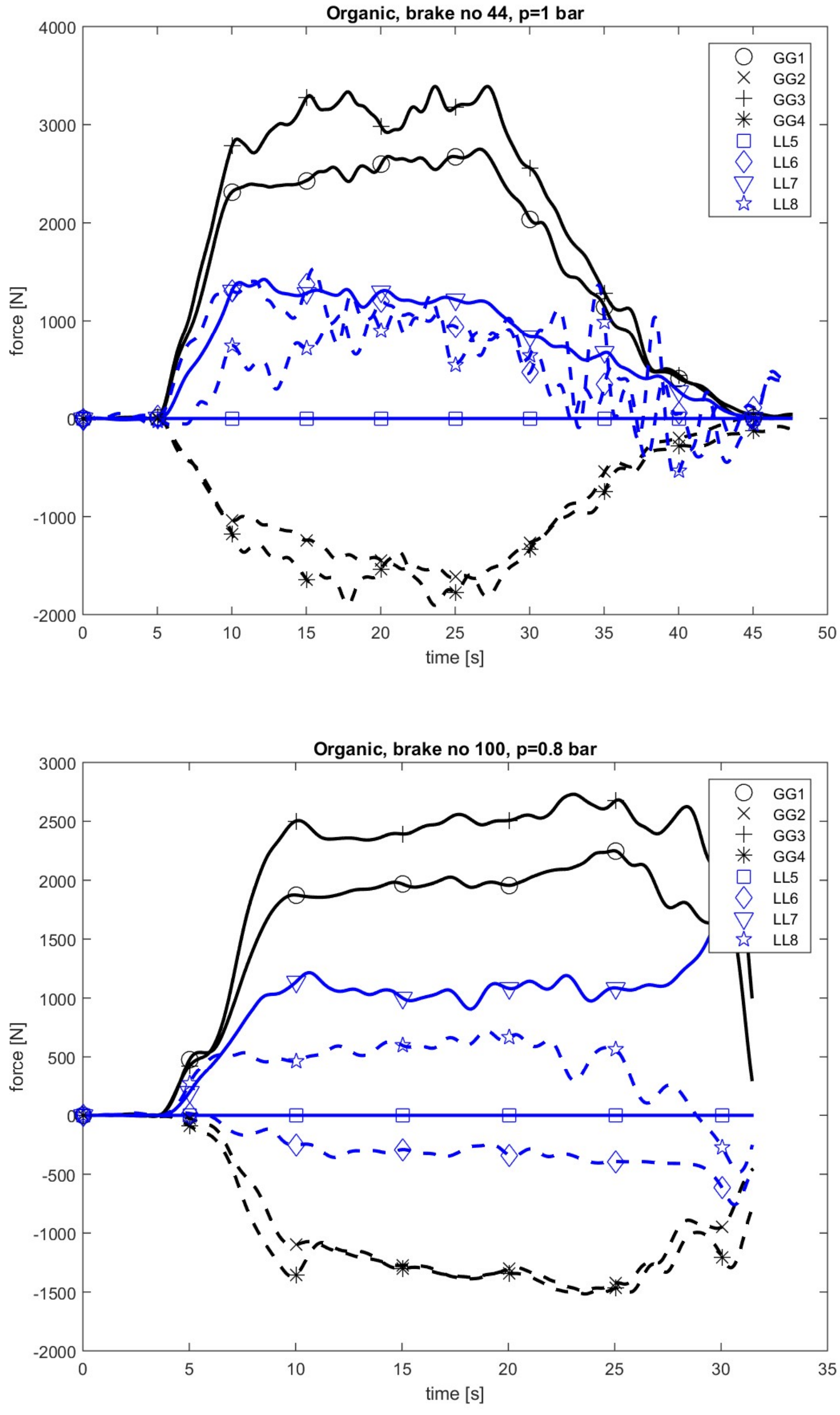

Figure 21 Two examples of time variation of forces for brake cycles with a high time delay until onset of friction forces for organic composite brake blocks.

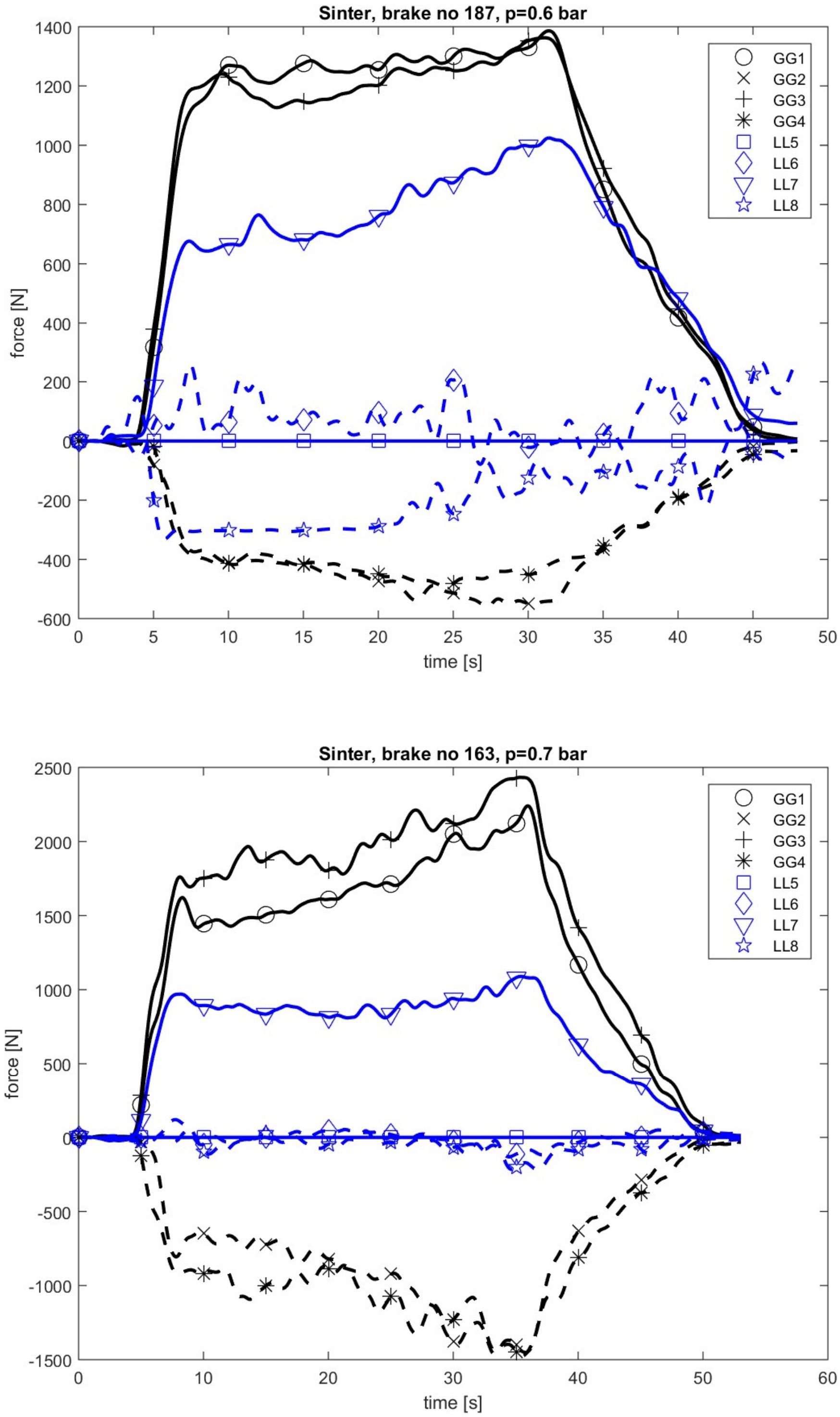

Figure 22 Two examples of time variation of forces for brake cycles with a high time delay until onset of friction forces for sinter brake blocks.